

# The METAS Photon-Beam Primary Standard Sealed Water Calorimeter

G. Stucki, R. Schafer, H. Quintel

Swiss Federal Office of Metrology and Accreditation (METAS)  
Bern-Wabern, Switzerland

## Abstract

In 2001 the METAS sealed water calorimeter became the Swiss primary standard for therapy-level photon-beam calibrations of the hospitals' reference dosimeters. Recently several modifications to the original design were made by the METAS and the use of the calorimeter was extended from  $^{60}\text{Co}$   $\gamma$ -radiation to high-energy photon beams with energies in the range from  $\text{TPR}_{20,10}=0.626$  to  $\text{TPR}_{20,10}=0.798$ .

The sensitivity of the AC bridge was doubled by moving one of the two thermistors into the opposite arm of the bridge. An electrical heater remotely controlled by a PID controller was installed to improve the long-term stability of the water temperature. For the measurements in the high-energy photon beams, two ionization chambers, used as monitors, were installed in the water tank behind the vessel. They are operated at 4 °C.

About two thousand  $^{60}\text{Co}$  irradiations have been carried out at the METAS so far, the uncertainty of the dose determination being 0.41 %. The calorimeter was bilaterally compared with the primary standards of the BIPM. The standards were in agreement within the uncertainty of the comparison.

The calorimeter was also used to determine the  $k_Q$  for NE2611 and NE2571 type ionization chamber working standards for high-energy photon beams. The uncertainty of the  $k_Q$  values is typically 0.55 %. Differences up to 1.2 % between measured and calculated  $k_Q$  values were observed.

A future project is to measure the heat defect of different aqueous systems directly. The method would be based on the total absorption experiment developed at the METAS: an electron beam of known particle energy and known beam charge is fully absorbed in a calorimeter. The measured dose is compared to the dose derived from the known particle energy and the known number of absorbed electrons. The heat defect can be obtained directly from this comparison. It is anticipated that the uncertainty of the heat defect determination will be less than 0.2 %.

## 1. Introduction

In 2001 the METAS sealed water calorimeter became the Swiss primary standard for therapy-level photon-beam calibrations of the hospitals' reference dosimeters. The calorimeter was originally constructed by the National Research Council, NRC, as part of a collaborative agreement between the NRC and the METAS. The calorimeter design follows the original NRC sealed water calorimeter [1] and uses two thermistor probes within a sealed glass vessel containing high purity water to measure the absorbed dose to water at a point in a larger water phantom. Only the pure water system, saturated with  $\text{N}_2$  gas was used for the experiments described in this paper. The relation between the absorbed dose,  $D_W$  and the temperature rise in the water,  $\Delta T_W$ , is given by

$$D_W = \Delta T_W \cdot c_W \cdot k_C \cdot k_P \cdot k_{DD} \cdot \frac{1}{1 - k_{HD}}$$

where  $c_W$  is the specific heat capacity of water,  $k_C$  the correction for conductive heat transfer,  $k_P$  a correction for the perturbation of the radiation field by the glass vessel and the probes,  $k_{DD}$  a correction for the non-uniformity of the lateral dose profile and  $k_{HD}$  the correction for the heat defect. These correction factors have been described in detail in [1, 2].

Recently several modifications to the original design were made by the METAS and the use of the calorimeter was extended from  $^{60}\text{Co}$   $\gamma$ -radiation to high-energy photon beams with beam qualities in the range from  $\text{TPR}_{20,10}=0.626$  to  $\text{TPR}_{20,10}=0.798$ . This paper describes the present status of the calorimeter and presents the results from the measurements performed so far. Throughout this paper all uncertainties quoted refer to a coverage factor  $k=1$ .

## 2. The METAS Sealed Water Calorimeter

### 2.1. Overview of the Calorimeter

The main elements of the calorimeter are shown schematically in Figure 1. The water is held in a PMMA tank, 30 cm on each side. The exterior walls of the tank are insulated with 5 cm thick Styrofoam. On the inner side of the Styrofoam there is an aluminized Mylar foil which is used as an inner electrical shield connected to earth. A magnetic stirrer for agitating the water between the measurements is built into the bottom of the tank. The lid of the tank contains several holes through which calibrated platinum resistor probes (Pt100) are inserted to measure the water temperature. The window of the tank through which the radiation enters is machined down to 3 mm over an area of 12 cm by 12 cm. The window is thermally isolated with a removeable, 5 cm thick Styrofoam plate with an electrical shielding on the inner side. The calorimeter phantom is enclosed in an insulated wooden box, 85 cm on each side, in which the temperature of the air circulating around the tank is stabilized to about 1.5 °C using fans and a heat exchanger. The cooling fluid can also be made to pass through a heat exchanger in the water tank so as to accelerate the process of reaching the operating temperature of 4 °C. The temperature of the cooling air is measured with a Pt100 probe and controlled by an external PID controller using an electrical heater which is mounted between the 2 wings of the heat exchanger. The wooden box has a Styrofoam insulation which in turn has an aluminized Mylar foil on its outer side. This foil acts as a second electrical shield.

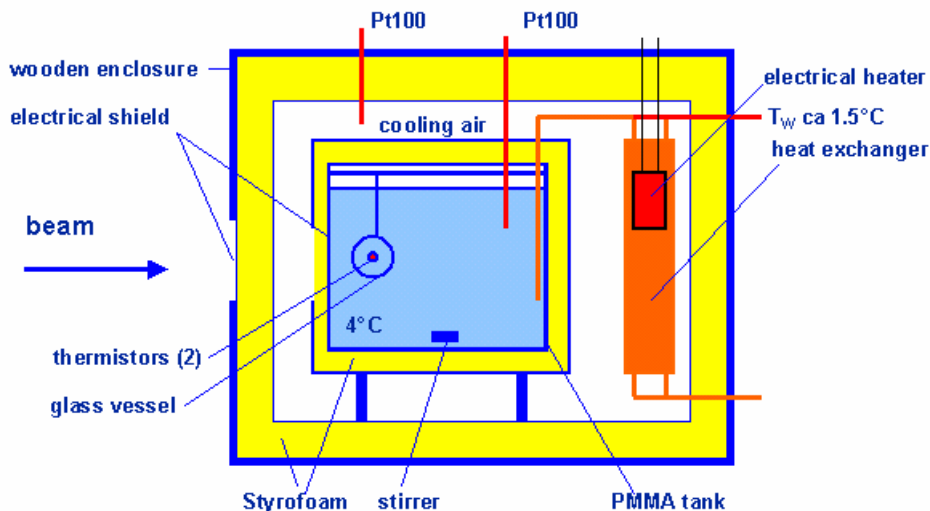


Figure 1. Side view of the METAS sealed water calorimeter used in  $^{60}\text{Co}$  beams. The drawing is not to scale. The principal elements of the calorimeter are labelled on the drawing.

## 2.2. Glass Detection Vessel

The temperature increase due to an irradiation is measured in the centre of a cylindrical glass vessel which is designed to isolate a small volume of high purity water from the water in the rest of the phantom. A typical glass vessel is shown in Figure 2. It consists of a central cylindrical portion, about 75 mm long. Threaded fittings on the end pieces hold the 2 thermistor probes (on the central axis of the vessel) in place. The vessel is mounted in the water tank on an adjustable slide so that its position along the beam axis can be varied.

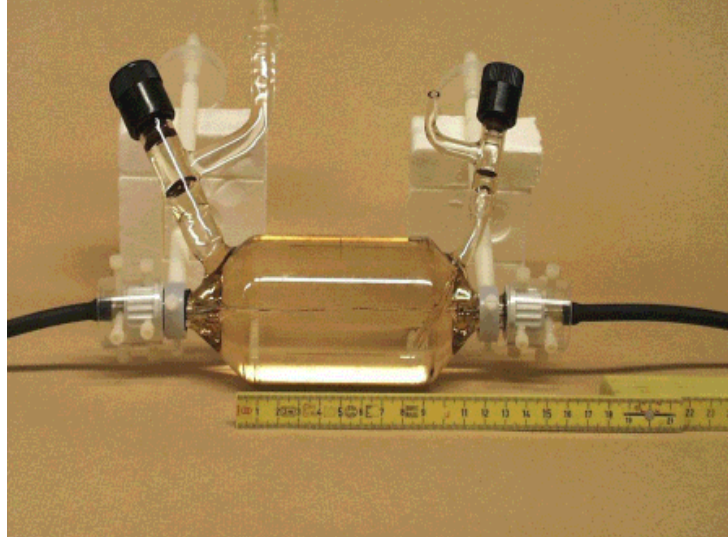


Figure 2. The glass detection vessel with the two thermistor probes aligned in the centre.

## 2.3. Thermistor Probes

A main requirement for calorimetry is that the thermistor probes accurately measure temperature changes. The approximate relationship between the thermistor resistance,  $R$  and the absolute temperature,  $T$ , is given by

$$R = R_0 \cdot e^{\beta(1/T - 1/T_0)}$$

where  $R_0$  is the resistance at the temperature  $T_0$  (25 °C) and  $\beta$  is a constant. The thermistor sensitivity,  $S$ , defined by

$$S = \frac{\Delta R}{R} \cdot \frac{1}{\Delta T}$$

where  $\Delta R$  is the change in resistance due to a temperature change of  $\Delta T$ , is then given by

$$S = -\frac{\beta}{T^2}$$

Accurate knowledge of a measured temperature change requires accurate knowledge of the thermistor constant,  $\beta$ . Domen [3] has reported significant changes in  $\beta$  with time, thus emphasizing the importance of routine checking of the thermistor constant  $\beta$ . The thermistors used at METAS were regularly calibrated against calibrated Pt100 in the temperature region from -4 °C to 12 °C.

## 2.4. Electronics

The circuit to measure the change in thermistor resistance is based on a four-arm AC bridge, operating at a frequency of 21.5 Hz. The output voltage from the bridge is measured using a commercial Lock-in amplifier. The bridge circuit, as well as the rest of the electronics used with the calorimeter, are shown in Figure 3.

The two thermistor probes (NTC1 and NTC2) are in the opposite arms of the bridge. The Lock-in amplifier and the two resistor decades (Burster decades) can be controlled and read out remotely by means of a GPIB bus. The platinum probes, which are used for temperature monitoring, are connected to a remotely controlled scanning system based on a Keithley 2001 multimeter equipped with a scanner card. The Labview software allows the bridge to be balanced, the characteristics of the Lock-in amplifier to be changed and the acquisition of the data. The stirrer as well as the PID controller are both only manually controlled.

At the operation temperature of 4 °C the resistance of the thermistors is about 10 k $\Omega$ . The response of the bridge per unit change in thermistor resistance is obtained by changing the resistance of the decade boxes by a known amount.

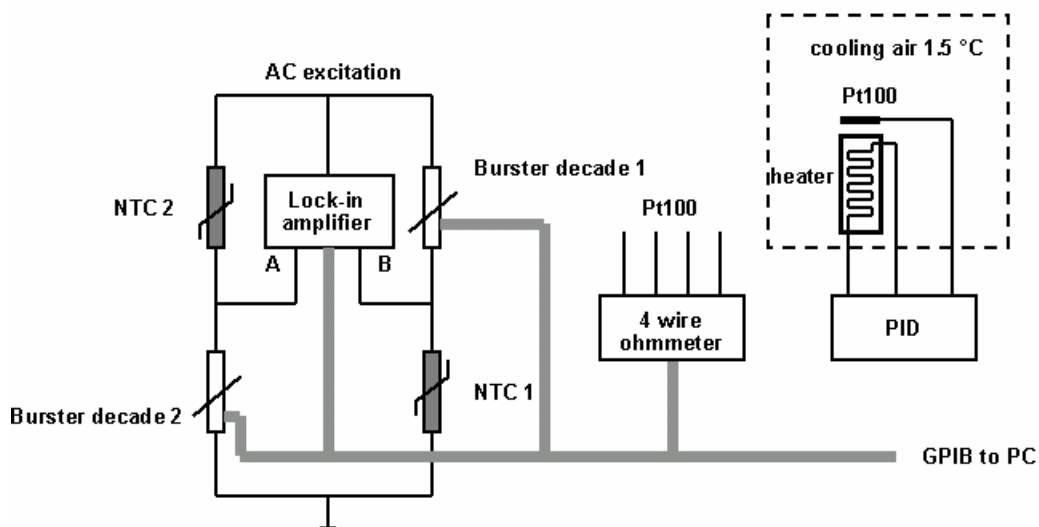


Figure 3. Bridge circuit and PID controller. The lock-in amplifier, the decade boxes and the 4 wire ohmmeter can all be controlled and read out remotely.

## 3. Determination of absorbed dose

### 3.1. Calorimeter used in a $^{60}\text{Co}$ beam

For determining the dose or dose rate at the reference point in a  $^{60}\text{Co}$  beam the calorimeter is used with the set-up described in paragraph 2.1. All measurements are done at 4 °C using an irradiation time of 120 s with a pre- and postirradiation drift time of 120 s. A General Electric Alcyon II  $^{60}\text{Co}$  unit is used for the irradiations with a field size of 10 cm by 10 cm at a depth in water of 5  $\text{gcm}^{-2}$ . The source to detector distance is 1 m.

An indirect comparison of the METAS calorimeter and the primary standard of the BIPM has been carried out in  $^{60}\text{Co}$   $\gamma$ -radiation. The comparison was carried out using four ionization chambers belonging to the METAS as transfer instruments. This comparison is described in Reference [3].

### 3.2. Calorimeter used in high-energy photon beams

The water calorimeter used in high-energy photon beams is essentially the same as the one used in  $^{60}\text{Co}$  beams, but in addition two ionization chambers used as monitors were inserted downstream as shown in Figure 4. The monitors are necessary because the dose rate of the beam depends on the accelerator beam current which can vary with time. The internal transmission chambers of the treatment head are used to control the beam positioning but are not stable enough to be used for absolute dosimetry. A M22 microtron with a conventional treatment head producing clinical beams with a field size of 10 cm by 10 cm at a depth in water of  $10 \text{ gcm}^{-2}$  is used. The source to detector distance is 1 m.

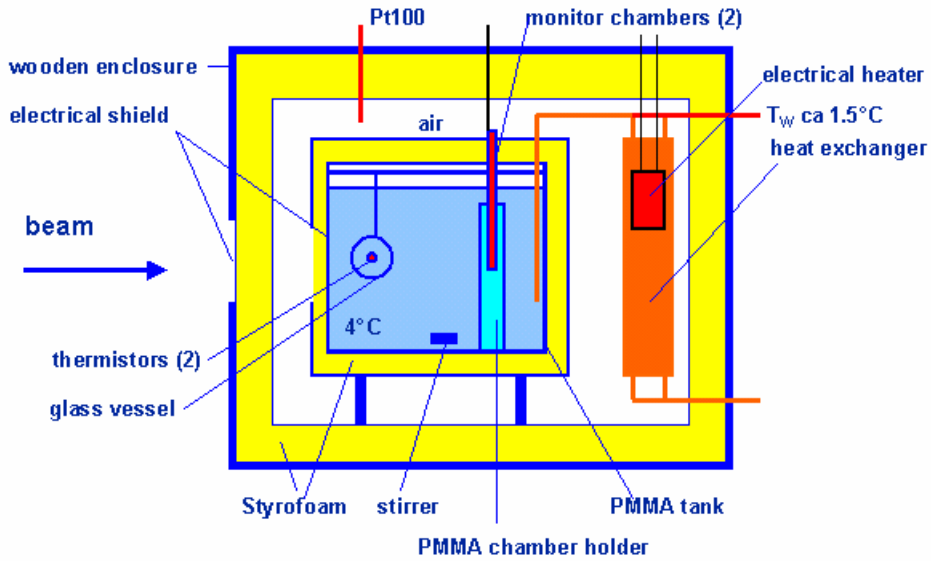


Figure 4. Side view of the METAS sealed water calorimeter used in high-energy photon beams.

In a first stage the calorimeter vessel is used to measure the monitor factor, MF, which is the ratio of the dose,  $D_{w,Q}$ , measured with the calorimeter vessel at the radiation quality Q, to the reading of the monitor chambers

$$\text{MF} = \frac{D_{w,Q}}{M_{m,Q}^C}$$

where  $M_{m,Q}^C$  is the monitor reading when measuring with the vessel at the radiation quality Q. The calorimeter and thus the monitors operated at 4 °C in this stage.

The monitor factor is used to calibrate a working standard ionization chamber in a second step, where the vessel is replaced by the chamber to be calibrated and the temperature of the water is increased to 20 °C. The calibration coefficient of the working standard,  $N_{w,Q}$ , is then given by

$$N_{w,Q} = \text{MF} \cdot \frac{M_{m,Q}^{\text{ws}}}{M_{m,Q}^C} \cdot f_{4,20}$$

where  $M_{m,Q}^{WS}$  is the monitor reading when measuring with the working standard at the radiation quality  $Q$ . In this second step, the monitors operate at 20 °C and the factor  $f_{4,20}$  corrects for any differences in the monitor response at 4 °C and 20 °C, respectively. The monitor chambers are mounted at a fixed geometrical depth in water. The measurements with the vessel (first stage) are performed at 4 °C, whereas those with the chamber (second stage) are done at 20 °C. The equivalent depth in water in  $gcm^{-2}$  is therefore different in the two stages due to a differing water density. The factor  $f_{4,20}$  corrects for this difference and also for the different beam perturbation of the vessel and the chamber, respectively.  $F_{4,20}$  has to be determined experimentally for each chamber type and each radiation quality. Although the correction is usually very close to unity it is nevertheless one of the major contributions (0.32 %) to the total uncertainty of the calibration coefficient (0.65 %).

## 4. Results and discussion

### 4.1. Thermistor long term stability

The results for  $\beta$ , evaluated at 4 °C, are summarized in Figure 5. Plotted are the thermistors constants  $\beta$ , normalized to their respective mean value  $\langle\beta\rangle$  for the 4 probes #21 (diamonds), #22 (squares), #23 (triangles) and #24 (circles). All measurements performed in the period of 5 years, from August 1998 to July 2003, were included. Thermistors #21 and #23 were mechanically damaged during the handling and are therefore no longer in use. The maximum standard deviation for the constant  $\beta$  (probe #21) is 0.02%.

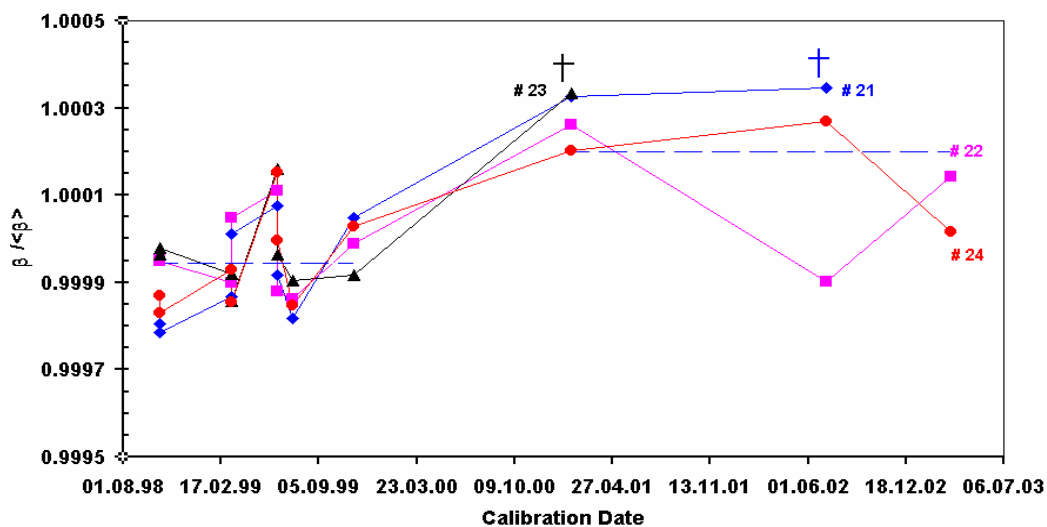


Figure 5. Thermistor longterm stability. The two broken lines indicate the mean of  $\beta / \langle\beta\rangle$  separately calculated for the two periods from August 1998 to May 1999 and September 2000 to July 2003, respectively. Plotted are the thermistors constants  $\beta$ , normalized to their respective mean value  $\langle\beta\rangle$  for the 4 probes #21 (diamonds), #22 (squares), #23 (triangles) and #24 (circles)

In 2000 the calibration set-up was slightly changed. A heat exchanger (closed loop) was introduced in the dewar where the calibration was done and the thermistors, when being calibrated, are no longer in direct contact with the circulating water of the temperature bath. This set-up better simulates the calorimeter measurement conditions where the probes are in stagnant water (in the vessel). So the transport of the probe's excess heat due to self-heating to the surrounding water is slightly different. This effect results in a small increase of  $\beta$  of

about 0.026 %, observed in the calibrations after September 2000. The broken lines in Figure 5 indicate the mean of  $\beta/\langle\beta\rangle$ , calculated for the two periods from August 1998 to May 1999 and from September 2000 to July 2003, respectively. The changes of  $\beta$  are not significant and no significant dose or time dependence such as reported by Domen in Reference [4] was observed for our thermistor probes.

#### 4.2. Dose rate in a $^{60}\text{Co}$ beam

Figure 6 shows the response of the calorimeter to  $^{60}\text{Co}$   $\gamma$ -radiation at a dose rate of 0.74 Gy/min. The voltage change was 7.64  $\mu\text{V}$ , which corresponds to a temperature rise of 0.35 mK. The pre-irradiation drift (magnified) is shown on the left and refers to the right scale axis. The peak-to-peak noise is about 50 nV.

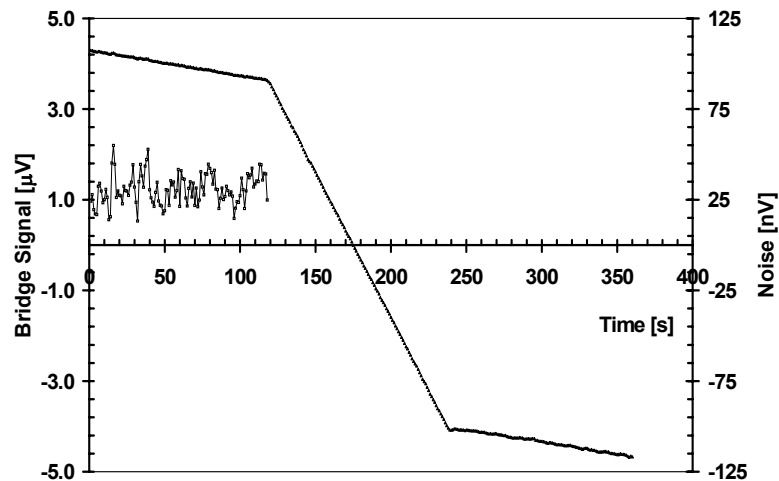


Figure 6. Sealed water calorimeter run (120 s) obtained using  $^{60}\text{Co}$   $\gamma$ -radiation at a dose rate of 0.74 Gy/min.

Figure 7 summarizes the results of 90 irradiation runs, grouped into 6 series of 15 consecutive measurements each and plotted as a function of the total absorbed dose.

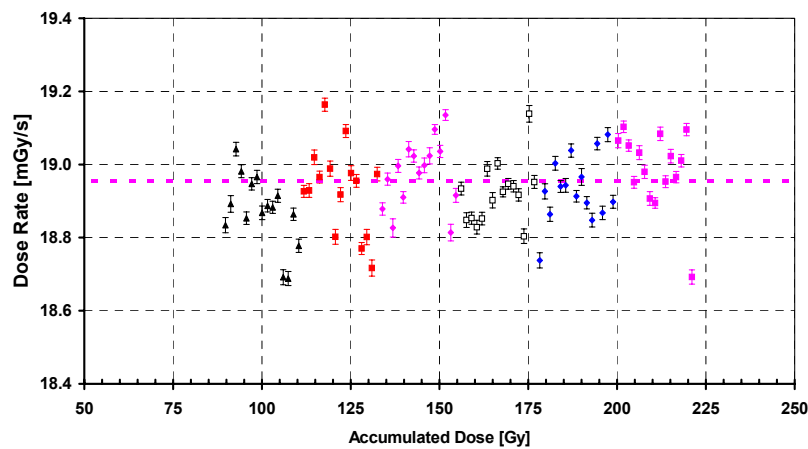


Figure 7. Dose rate in the  $^{60}\text{Co}$  beam at 1 July 1999 determined with the water calorimeter. The broken line indicate the mean dose rate referring to 1 July 1999.

Between each series sufficient time was allowed for the calorimeter to reach temperature equilibrium (typically 90 minutes). The mean dose rate indicated as broken line and referring to the reference date 1 July 1999 was 18.937 mGy/s with a standard deviation of 0.21 %. The uncertainty bars on the plot refer to type A uncertainties only. No significant dependence of the dose rate on the total accumulated dose could be observed.

The dose rate corrected for decay to 1 July 1999 was regularly determined in the period from October 2000 to October 2002. Table 1 shows the results for the dose rate determinations, which agreed well within the combined standard uncertainty of 0.41 %.

Table 1. Dose rate for  $^{60}\text{Co}$  referring to 1 July 1999, measured over a period of 2 years

| Date         | Dose rate [mGy/s] | Uncertainty in % |
|--------------|-------------------|------------------|
| October 2000 | 18.912            | 0.41             |
| May 2001     | 18.948            | 0.41             |
| October 2002 | 18.937            | 0.41             |

The uncertainty budget for the absorbed dose to water,  $D_w$ , at  $^{60}\text{Co}$   $\gamma$ -radiation is given in Table 2. The combined standard uncertainty of 0.41 % is dominated by the heat defect, which contributes 0.30 %.

Table 2. Combined relative standard uncertainty of  $D_w$ .  $S_i$  represents a type A relative standard uncertainty estimated by statistical means;  $u_i$  represents a type B relative standard uncertainty estimated by other means.

|   | Uncertainty in % |       |
|---|------------------|-------|
|   | $S_i$            | $u_i$ |
| Specific heat of water $c_w$ :                    |                  | 0.01  |
| Heat defect $k_{HD}$ :                            |                  | 0.30  |
| Conductive heat transfer $k_C$ :                  |                  | 0.15  |
| Field perturbation $k_P$ :                        | 0.05             |       |
| Thermistor calibration:                           | 0.20             |       |
| Measurement of $\Delta T_w$ :                     | 0.06             |       |
| Beam profile correction $k_{DD}$ :                |                  | 0.02  |
| Source surface distance:                          |                  | 0.02  |
| Depth in water:                                   |                  | 0.10  |
| Quadratic summation:                              | 0.21             | 0.35  |
| Combined relative standard uncertainty of $D_w$ : |                  | 0.41  |

An indirect comparison of the METAS calorimeter and of the standard of absorbed dose to water of the BIPM has been made at  $^{60}\text{Co}$   $\gamma$ -radiation. The results show that the METAS and the BIPM standards for absorbed dose are in agreement, yielding a comparison result of 1.0001 for the mean ratio (METAS/BIPM) of the calibration coefficients for the four transfer chambers, the difference from unity being within the combined standard uncertainty of the comparison,  $u_c = 0.54$  %.

#### 4.3. Experimental $k_Q$ factors for NE2611 and NE 2571 ionization chambers at high-energy photon radiation

The response of the calorimeter, in terms of the monitor factor, to a high-energy photon beam is shown in Figure 8. The measurement was done at 4 °C using an irradiation time of 120 s

with a pre- and post-irradiation drift time of 120 s. The beam quality was  $TPR_{20,10} = 0.798$  and the dose rate was 2 Gy/min. The voltage change due to the irradiation was about 20  $\mu\text{V}$ , corresponding to a temperature rise of 1 mK.

Figure 9 shows the pre-and post-irradiation drift curves. The peak-to-peak noise was 50 nV. The noise level was the same as in the  $^{60}\text{Co}$  beam and the measurements were therefore not affected by any high frequency noise from the accelerator. The signal to noise ratio is a factor of 3 better compared to the  $^{60}\text{Co}$  measurements. This is due to the higher dose rate and - since the irradiation time is the same - due to a higher dose.

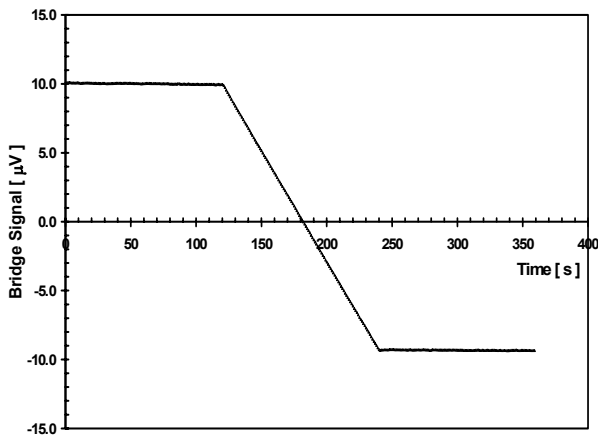


Figure 8. Calorimeter run (120 s) obtained using a high-energy photon beam with a beam quality of  $TPR_{20,10}=0.798$ .

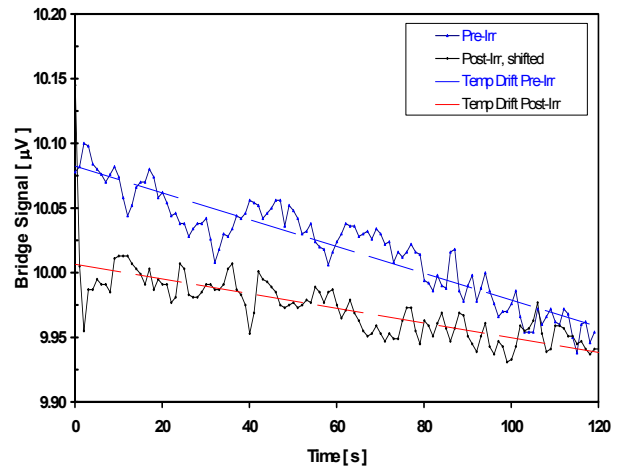


Figure 9. Sealed water calorimeter run pre - and post irradiation drift time. The broken lines indicate linear fits to the drift curves.

Figure 10 summarizes the results, expressed in terms of the monitor factor, of 80 irradiation runs, grouped into 10 series of 8 consecutive measurements each and plotted as a function of the total absorbed dose.

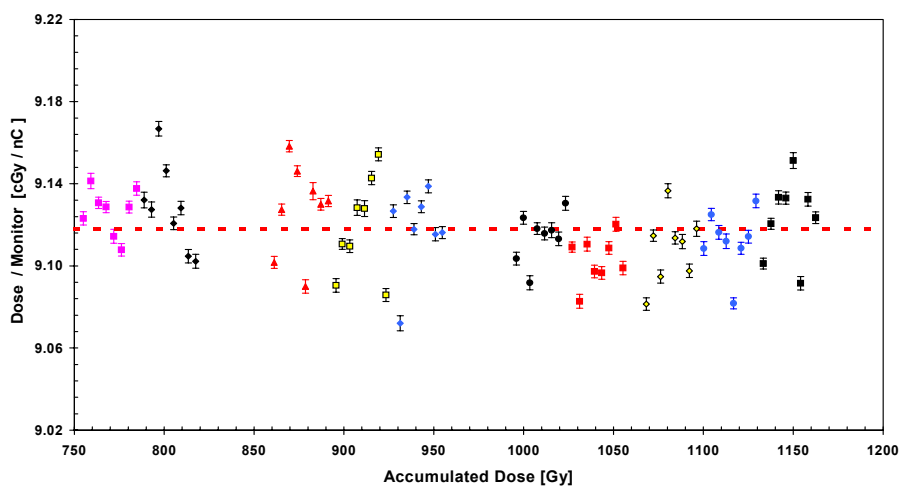


Figure 10. Monitor factor determined in a high-energy photon beam with a radiation quality of  $TPR_{20,10}=0.798$  as a function of the accumulated dose. The different symbols represent the groups of 8 consecutive measurements. The broken line indicate the mean monitor factor which was 9.118 cGy/nC.

Because of the higher dose rate only 8 irradiations could be done in a series. Between each series sufficient time was allowed for the calorimeter to reach temperature equilibrium (typically 90 minutes). The mean monitor factor was 9.118 cGy/nC with a standard deviation of 0.21 %. The uncertainty bars on the plot refer to type A uncertainties only. No significant dependence of the dose rate on the total accumulated dose could be observed.

The beam quality correction factor  $k_Q$  is defined as the ratio of the absorbed dose to water calibration coefficient,  $N_{W,Q}$  at the quality  $Q$  to the same quantity at a reference quality, usually  $^{60}\text{Co}$

$$k_Q = N_{W,Q} / N_{W,\text{Co}}$$

This beam quality correction factor has been determined using the calorimeter to calibrate the ionization chambers in the  $^{60}\text{Co}$  beam and in 10 different high-energy photon beams. As beam quality specifier we used  $\text{TPR}_{20,10}$ . The beam qualities measured were between  $\text{TPR}_{20,10} = 0.626$  and  $\text{TPR}_{20,10} = 0.798$ . Figure 11 shows the mean values of  $k_Q$  at various photon beam qualities measured at the METAS for ionization chambers of the types NE2561/NE2611 and NE2571. Four chambers of each type were measured. The uncertainty of  $k_Q$  was 0.55 %. The solid lines are sigmoidal fits to calculated  $k_Q$  values taken from Table 15 of the IAEA TRS 398, Reference [5]. Up to a  $\text{TPR}_{20,10}$  of about 0.7 the measured  $k_Q$  agree well with the calculated values. At a  $\text{TPR}_{20,10}$  of 0.639 the measured  $k_Q$  is slightly higher than unity for both chamber types. This could be explained by an error in the measurement of the  $f_{4,20}$  correction factor (with an uncertainty of 0.32 %) which has a component that is measured just once for a particular beam quality and all measurements at this quality are thus correlated.

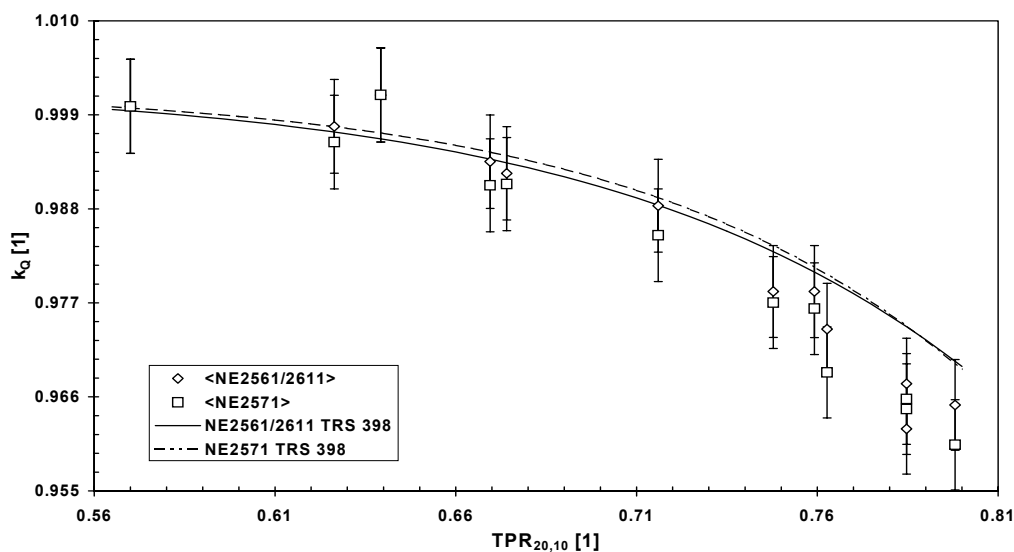


Figure 11. Experimental  $k_Q$  at various photon beam qualities for chambers of type NE2561/2611 (diamonds) and NE2571 (squares). The lines indicate the calculated  $k_Q$  for NE2561/NE2611 (full line) and NE2571 (broken line).

Above  $\text{TPR}_{20,10}$  of 0.7 the measured  $k_Q$  are generally lower than the calculated value. The maximum deviation is 1.2 %. The reason for this deviation is not clear. The measured  $k_Q$  were not corrected for the polarity effect since at the METAS only negative polarity was used. But for chambers of type NE2561/NE2611 and NE2571 the polarity correction factor is expected to be less than 0.15 % which is much less than the reported deviation of 1.2 %. The standard deviation of the measured  $k_Q$  values for a particular chamber type at one energy is typically

0.2 %. Similar deviations of the measured  $k_Q$  at higher energies were also observed at other laboratories, like the NPL, as shown in Figure 5 of Reference [5], where a deviation of about 0.6 % at a  $TPR_{20,10}$  of 0.79 is reported.

At the METAS two different beams, both having a  $TPR_{20,10}$  of 0.785, were measured. Their nominal energy is different, one quality is produced with an 18 MeV electron beam the other one with a 20 MeV electron beam. Due to different beam filtrations they both have the same  $TPR_{20,10}$ .

## 5. Future project

There is still an ongoing debate on the uncertainty of the heat defect of water. Values for the uncertainty of the heat defect used by different laboratories vary from 0 % to about 0.3 %. These figures are mainly based on simulations using widely accepted models for the radiolysis of water but in some cases they are not directly supported by experiments.

A future METAS project is to measure the heat defect of different aqueous systems directly. The method would be based on the total absorption experiment developed at the METAS and described in Reference [6]. The set-up is shown in Figure 12. An electron beam of known particle energy,  $E_e$ , and known number of electrons,  $N$ , is fully absorbed in a volume of water of mass  $m$ . The electron energy is measured using a magnetic spectrometer and the number of electrons by means of a beam charge monitor.

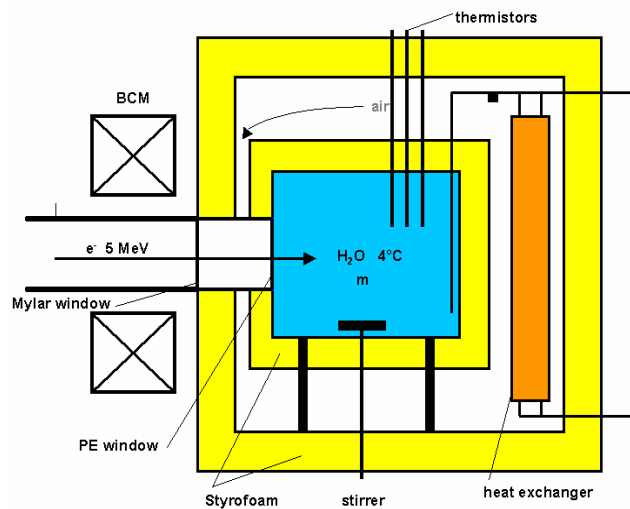


Figure 12. Set-up of the planned total absorption experiment for measuring the heat defect. The drawing is not to scale. The electron beam enters from the left through the Mylar window. To minimize the corrections to be applied the size of the vessel containing the water at 4 °C is chosen such that all electrons of the beam are stopped and absorbed in the water.

The measured dose,  $D_w$ , is compared to the dose,  $D_d$ , derived from the known particle energy, the known number of absorbed electrons and the mass of the water. The heat defect,  $k_{HD}$ , can be obtained directly from this comparison:

$$D_w = \frac{\Delta T \cdot c_w}{1 - k_{HD}} \quad D_d = \frac{E_e \cdot N}{m}$$

$$k_{HD} = 1 - \frac{\Delta T \cdot c_w \cdot m}{E_e \cdot N}$$

For clarity all correction factors except that for heat defect are omitted in these equations. The dose  $D_D$  must be corrected for losses due to Bremsstrahlung and backscattering and for energy losses in the entrance foils. These corrections will be determined by Monte Carlo simulations. As an electron energy as low as 5 MeV will be used, the Bremsstrahlung correction is expected to be around 2.1 % and the total correction about 2.7 %. Due to a high beam current and thus a high dose the temperature rise can be more than 100 mK and therefore the uncertainty of the  $\Delta T_W$  is as low as 0.05 %. The resulting uncertainty of  $k_{HD}$  is expected to be about 0.2 %. The corresponding uncertainty budget is shown in Table 3.

Table 3. Estimated relative standard uncertainty of  $k_{HD}$  for the future total absorption experiment

|   | Uncertainty in % |
|---|------------------|
|   | $u_i$            |
| Specific heat of water $c_W$ :  | 0.01             |
| Electron energy $E_e$ :   | 0.10             |
| Number of electrons $N$ :   | 0.10             |
| Mass of the water $m$ :   | 0.01             |
| Measurement of $\Delta T_W$ :   | 0.05             |
| Bremsstrahlung correction:  | 0.10             |
| Energy losses and backscattering:                                     | 0.10             |
| <b>Combined relative standard uncertainty of <math>k_{HD}</math>:</b> | <b>0.20</b>      |

## 6. Conclusions

The use of the METAS sealed water calorimeter operated at 4 °C was successfully extended from  $^{60}\text{Co}$   $\gamma$ -radiation to high-energy photon radiation. It is now the Swiss primary standard for the absorbed dose to water at  $^{60}\text{Co}$   $\gamma$ -radiation and at high-energy photon beams with beam qualities between  $\text{TPR}_{20,10} = 0.626$  and  $\text{TPR}_{20,10} = 0.798$ .

For ionization chambers of the types NE2561/NE2611 and NE2571 calibration coefficients and  $k_Q$  values have been measured and compared with calibration coefficients determined by other laboratories and with calculated  $k_Q$  values. The agreement for  $^{60}\text{Co}$  is excellent. For high-energy photon beams up to a  $\text{TPR}_{20,10}$  of about 0.7 the experimental  $k_Q$  values agree well with the calculated  $k_Q$  taken from Reference [5]. Above a  $\text{TPR}_{20,10}$  of about 0.7 the experimental  $k_Q$  values are up to 1.2 % lower than the calculated  $k_Q$ . The reason for this deviation is not clear and remains to be investigated.

## 7. References

- [1] Medin, J., Seuntjens, J., Klassen, N., Ross, C.K., Stucki, G., “The OFMET sealed water calorimeter”, Recent Advances in Calorimetric Absorbed Dose Standards (Proc. Workshop Teddington, UK, 1999), Rep. CIRM 42 (Williams, A.J., Rosser, K.E., Eds), National Physical Laboratory, Teddington, UK (2000) 65–73.
- [2] Ross C. K., Seuntjens, J., Klassen, N., Shortt K. R., “The NRC sealed water calorimeter: correction factors and performance”, Recent Advances in Calorimetric Absorbed Dose Standards (Proc. Workshop Teddington, UK, 1999), Rep. CIRM 42 (Williams, A.J., Rosser, K.E., Eds), National Physical Laboratory, Teddington, UK (2000) 90-102.
- [3] Allisy-Roberts, P., Burns, D., Stucki, G., Comparison of the Standards of Absorbed dose to Water of the METAS, Switzerland and the BIPM for  $^{60}\text{Co}$   $\gamma$  rays, Rapport BIPM-03/02 (2003).

[4] Domen S. R., "A sealed water calorimeter for measuring absorbed dose", J. Res. Nat. Bur. Stand. 99, 121-141 (1994)

[5] IAEA, „Absorbed dose Determination in External Beam Radiotherapy, An International Code of Practice for Dosimetry Based on Standards of Absorbed Dose to Water“, Technical Report Series No. 398, Vienna 2000.

[6] Stucki G., Schafer R., Brunshwig O., Quintel H., "The METAS Electron-Beam Primary Standard Chemical Dosimeter", Presentation in this workshop

## **Discussion**

*Malcolm McEwen* – Gerhard, you've compared your measured  $k_Q$ s with TRS 398, but how do they compare with other measured values, like the NPL  $k_Q$  data or what Hugo Palmans did at Gent ?

*Gerhard Stucki* – Well, I don't know about the  $k_Q$  from Gent, I can't recall these figures at the moment, but our  $k_Q$  agree(s) pretty well with the one from the NPL, at least within the uncertainties which are estimated.

*Hugo Palmans* – There was a publication from Pedro Andreo summarizing a number of experimental  $k_Q$  values, and I think that for the NE2571 chamber it was fairly similar. We saw an overall picture of experimental  $k_Q$  values which were about 1% lower than the calculated ones at high TPR values. But for the NE2561 it was not the case, I think. They were in agreement with calculated values, in general.

*Gerhard Stucki* – Well, generally the  $k_Q$  of the NE2611 is a bit closer to the one from the code, (according to) our measurements (in this) case.

*Malcolm Millar* - Do the Swiss hospital physicists use your measured values of  $k_Q$ , or do they use the TRS 398 value?

*Gerhard Stucki* – They use the Swiss protocol. This protocol is quite new and it complies fully with the Agency code.

*David Webb* – OK, but you use the  $k_Q$  that you supply?

*Gerhard Stucki* – Yes.

*John Boas* – With the 2561 and the 2611s, did you notice any difference at, say, 18 MV in terms of  $k_Q$ ?

*Gerhard Stucki* – No.

*John Boas* – No. How many chambers of each type did you use?

*Gerhard Stucki* – At least five of each type.

*David Webb* – You've got to put moisture in the chambers to make them different, I believe.

*Gerhard Stucki* – Unfortunately we didn't see any difference.

*Russell Thomas* – Fortunately!

*Malcolm McEwen* – I'm just going to make a comment. There have been a number of references to the '99 workshop. It might be worth making clear to people that all the proceedings from that are on the NPL website for download, if people are interested.

*Robert Huntley* – Gerhard, with the computer controlled decade boxes, what's the resolution of those in ohms? What's the smallest step size?

*Gerhard Stucki* – A hundredth of an ohm.

*Robert Huntley* – Point 01, OK. And do you have any problem with contact resistance with those? Do you know what the contacts are? How they're done?

*Gerhard Stucki* – I don't recall it at the moment, but we check this box regularly in the electrical standard(s) lab, and we couldn't find any deviation with time of the contacts.

*Robert Huntley* – So they're reproducible at the point 01 ohm level?

*Gerhard Stucki* – Yes.

*Robert Huntley* – That's excellent, I'd like to know where they come from, if you could supply me that information later?

*David Webb* – I'm curious about your  $f_{4,20}$  correction ... You've done an empirical measurement of that correction, you haven't done any calculations as to what you think it ought to be?

*Gerhard Stucki* – No, these are only experimental results.